Diet and Adaptive Evolution of Alanine-Glyoxylate Aminotransferase Mitochondrial Targeting in Birds

Bing-Jun Wang,[1] Jing-Ming Xia,[1] Qian Wang,[1] Jiang-Long Yu,[2] Zhiyin Song,[2] and Huabin Zhao ![ORCID] *,[1]

[1]Department of Ecology, Hubei Key Laboratory of Cell Homeostasis, College of Life Sciences, Wuhan University, Wuhan, China
[2]Department of Cell Biology, Hubei Key Laboratory of Cell Homeostasis, College of Life Sciences, Wuhan University, Wuhan, China

*Corresponding author: E-mail: huabinzhao@whu.edu.cn.
Associate editor: Claudia Russo

Abstract

Adaptations to different diets represent a hallmark of animal diversity. The diets of birds are highly variable, making them an excellent model system for studying adaptive evolution driven by dietary changes. To test whether molecular adaptations to diet have occurred during the evolution of birds, we examined a dietary enzyme alanine-glyoxylate aminotransferase (AGT), which tends to target mitochondria in carnivorous mammals, peroxisomes in herbivorous mammals, and both mitochondria and peroxisomes in omnivorous mammals. A total of 31 bird species were examined in this study, which included representatives of most major avian lineages. Of these, 29 have an intact mitochondrial targeting sequence (MTS) of AGT. This finding is in stark contrast to mammals, which showed a number of independent losses of the MTS. Our cell-based functional assays revealed that the efficiency of AGT mitochondrial targeting was greatly reduced in unrelated lineages of granivorous birds, yet it tended to be high in insectivorous and carnivorous lineages. Furthermore, we found that proportions of animal tissue in avian diets were positively correlated with mitochondrial targeting efficiencies that were experimentally determined, but not with those that were computationally predicted. Adaptive evolution of AGT mitochondrial targeting in birds was further supported by the detection of positive selection on MTS regions. Our study contributes to the understanding of how diet drives molecular adaptations in animals, and suggests that caution must be taken when computationally predicting protein subcellular targeting.

Key words: alanine-glyoxylate aminotransferase, diet, mitochondrial targeting, birds.

Introduction

Birds belong to the most species-rich class of tetrapod vertebrates, represented by over ten thousand extant species (Gill and Donsker 2013). Birds typically have higher basal metabolic rates than other vertebrates, thus they must consume enough food each day to meet their energy requirements. Avian diets are extraordinarily diverse and include virtually every type of food, such as fruits, flowers, pollen, nectar, carrion, insects, fishes, and other small animals (Lovette and Fitzpatrick 2016). Many bird species are specialists that are highly selective and adept at eating one or few specific types of food, whereas others are generalists that rely on a wide variety of prey (Burin et al. 2016). There is overwhelming evidence demonstrating that the feeding ecology of birds plays a crucial role in driving the evolution of their morphological, physiological and behavioral traits via adaptations specific to different food resources (O'Donnell et al. 2012; Abrahamczyk and Kessler 2015). For example, Darwin's finches of the Galápagos Islands represent one of the most recognized illustrations of feeding adaptation, wherein selection for particular foods has driven the evolution of beak size and shape (Grant 1999; Olsen 2017). However, in contrast to morphological adaptations, molecular adaptations to diverse diets in birds remain largely unexplored.

The liver enzyme alanine-glyoxylate aminotransferase (AGT) appears to show an evolutionary adaptation to diet in mammals (Ichiyama 2011). The intermediary metabolite glyoxylate can be converted to the metabolic end product oxalate, which can be toxic to mammals since too much oxalate in the urine could result in kidney stones (Danpure et al. 1989; Cochat and Rumsby 2013) (fig. 1A). Fortunately, the AGT enzyme is responsible for detoxifying glyoxylate by catalyzing the transamination of glyoxylate to glycine, thereby preventing glyoxylate from being converted to oxalate (Danpure 1997; fig. 1A). In carnivorous mammals, glyoxylate is mainly formed in mitochondria from hydroxyproline, which is the key component of collagen in animals (Neuman and Logan 1950; Maitra and Dekker 1964; Lowry et al. 1985; Takayama et al. 2003; fig. 1A). In herbivorous mammals, however, glyoxylate is mainly synthesized in peroxisomes by the oxidation of glycolate, an intermediate of photorespiration in plants (Harris and Richardson 1980; fig. 1A). Indeed, the tendency for AGT to target mitochondria in carnivorous mammals (including insectivores), to target peroxisomes in herbivorous mammals, and to target both peroxisomes and mitochondria in omnivorous mammals has been identified (Danpure et al. 1990; Danpure et al. 1994; Birdsey et al. 2005). Thus, the best place for AGT to detoxify glyoxylate may depend on diet: in carnivorous mammals, AGT targets
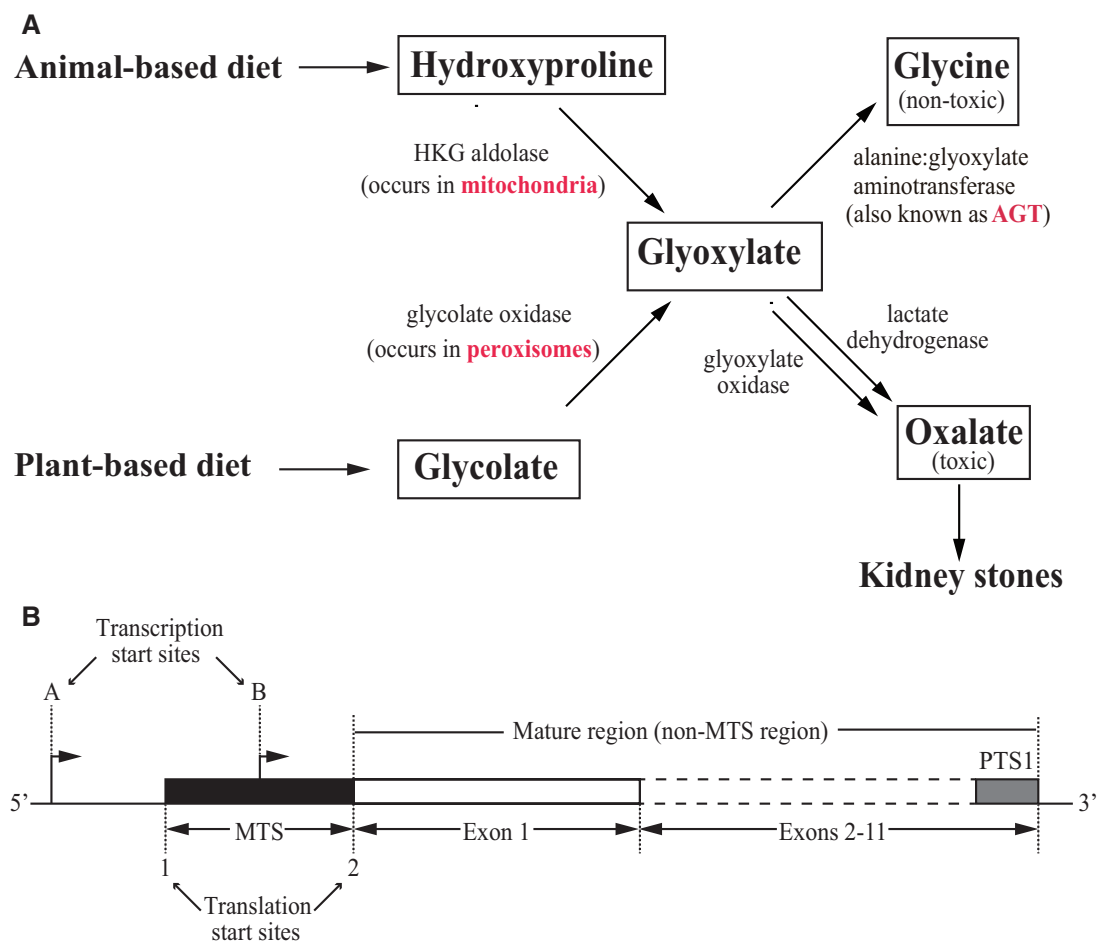
Fig. 1. Glyoxylate detoxification pathway and canonical structure of *AGT*. (*A*) Schematic to show the glyoxylate detoxification pathway and the putative relationship between diet and AGT. (*B*) Canonical structure of *AGT* with the MTS and mature regions indicated.

mitochondria, and in herbivorous mammals, it targets peroxisomes.

In all mammals examined to date, the liver enzyme AGT is encoded by a single-copy gene (*AGXT*, or *AGT*) (fig.1B; Birdsey et al. 2005). The full-length *AGT* gene contains 11 coding exons (as identified in the rat), and typically encodes an N-terminal mitochondrial targeting sequence (i.e., MTS) of 22 amino acids and a C-terminal type 1 peroxisomal targeting sequence (i.e., PTS1) of three amino acids (fig. 1B; Oda et al. 1987; Motley et al. 1995; Birdsey et al. 2005). In addition to the MTS region, AGT also has a nonMTS region, otherwise known as the mature region (fig. 1B). Splicing of the mature region produces the mature protein (Ichiyama 2011). Although both the MTS and PTS1 play important roles in the subcellular localization of AGT, the former is functionally dominant over the latter and thus AGT localization is largely determined by the MTS (Oatey, Lumb, Danpure 1996). AGT has two alternative transcription start sites and two alternative translation start sites (fig. 1B; Danpure 1997). If mutations in the MTS result in evolutionary loss of the upstream translation start site, AGT would be exclusively peroxisomal, as observed, for instance, in the guinea pig (Birdsey and Danpure 1998). Molecular genetic analyses of AGT evolution have been conducted extensively in the context of ecology

and dietary diversity in mammals (Holbrook et al. 2000; Birdsey et al. 2004; Birdsey et al. 2005; Liu et al. 2012). However, such analyses are scarce in birds, which show an extraordinary diversity of diets. Furthermore, experimental data on the subcellular location of AGT are rather limited in mammals and virtually unavailable in birds thus far. Hence, we also aimed to improve a previously developed cell-based functional assay for future use in birds and other vertebrates.

To test whether molecular adaptations to diverse diets have occurred in birds, we took advantage of the 48 avian genomes from the Avian Phylogenomics Project (http://avian.genomics.cn/en/; last accessed January 1, 2016), which include representatives from 34 of all 37 orders in the class Aves (Jarvis et al. 2014; Zhang et al. 2014). We characterized the *AGT* gene from these avian genomes, determined the mitochondrial targeting efficiency of AGT using an improved cell-based functional assay, and conducted molecular genetic analysis of AGT evolution in birds.

Results

AGT Identification and Sequence Alignment

By searching through 48 avian genome sequences, we were able to recover the 5′ flanking region of the *AGT* gene that
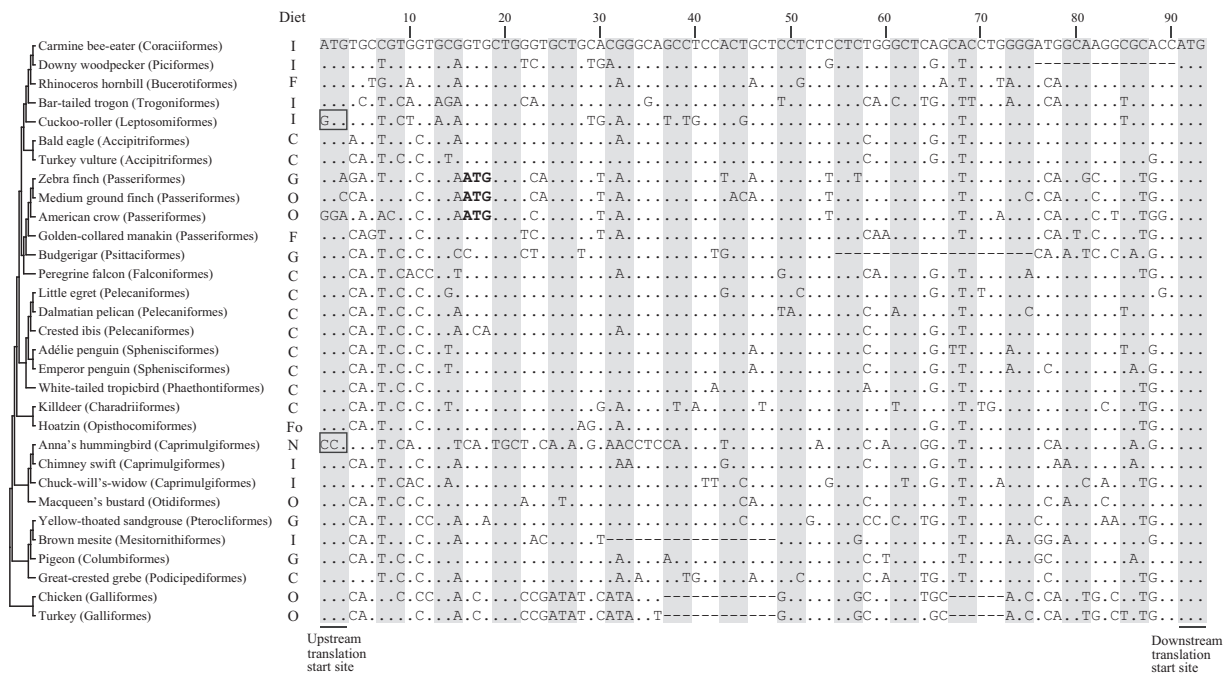
FIG. 2. Sequence alignment of avian MTSs. Boxed regions indicate nonfunctional MTSs caused by mutations in the upstream translation start sites. Bold font indicates putative translation start codons in three passerine species. Dietary information was taken from the EltonTraits 1.0 database. Abbreviations: I, insectivore; F, frugivore; C, carnivore; G, granivore; O, omnivore; Fo, folivore; N, nectarivore.

includes the MTS in 31 avian species (fig. 2). Of these, 14 species have a full-length *AGT* that contains both the MTS and mature regions (supplementary table S1, Supplementary Material online), the latter of which includes PTS1 and 11 coding exons. Unlike the much shorter MTS, the start and stop codons of the mature region span a long region containing 11 exons and 10 introns (fig. 1B). In our study, we are able to recover the 5′ flanking region of the translation start site 2 of AGT in 31 avian species (fig. 2). However, of the 29 species having an intact N-terminal MTS, we can obtain the complete sequence of 11 exons of AGT only in 14 species, due to genome incomplete sequencing. After aligning MTSs from the 31 species, missense mutations were detected in the upstream translation start site in the Anna's hummingbird and cuckoo-roller (fig. 2), suggesting that the MTS is nonfunctional and thus mitochondrial targeting has been lost in these two species. Although missense mutations were also observed in the upstream translational site in the three passerine birds (zebra finch, medium ground finch, and American crow), an alternative translational site was identified 15-bp downstream (fig. 2). We predicted that the three passerine birds may still have an intact MTS (fig. 2), which was tested in our subsequent functional assays. In total, the MTSs of 29 species appear to be intact and putatively functional. However, they are poorly conserved, with a length that varied from 23 to 30 amino acids (fig. 2).

After aligning the PTS1s from the 14 avian species with a full-length *AGT*, we found that, in contrast to the MTSs, these sequences are highly conserved (fig. 3). Specifically, the PTS1 (i.e., C-terminal tripeptide) in most birds terminated with SRL, except in the chimney swift, which terminated with SRM (supplementary fig. S1, Supplementary Material online).

Both SRM and SRL completely match the PTS1 consensus sequence (S/A/C-K/R/H-L/M; Gould et al. 1989; Swinkels et al. 1992). Furthermore, we identified additional PTS1s from eight reptiles, 21 mammals, and one frog through genome searches (supplementary tables S2 and S3, Supplementary Material online). Unlike birds, PTS1s in other species are not conserved, and in most cases do not match the consensus sequence (supplementary fig. S1, Supplementary Material online), suggesting that the sequence conservation of PTS1 is specifically required in birds.

Mitochondrial Targeting of AGT and Avian Diet

To compare the levels of mitochondrial targeting of AGT among birds, we first carried out computer prediction using the PSORT program (Nakai and Horton 1999). According to the PSORT prediction, AGT targeted to mitochondria is expected to have a PSORT score greater than zero (Nakai and Horton 1999; Marcotte et al. 2000). We hypothesized that bird species whose diet consisted of >50% meat (namely carnivores) may have an AGT that tends to target mitochondria. To our surprise, although PSORT scores closely match with diet in mammals (Birdsey et al. 2004; Liu et al. 2012), we detected widespread mismatches between PSORT scores and dietary preferences in birds (supplementary table S4, Supplementary Material online). These mismatches were found in 15 of the 29 species with an intact MTS; these mismatches arose either when a negative PSORT score was found in a carnivore, or a positive PSORT score was found in a herbivore (supplementary table S4, Supplementary Material online). For instance, the MTS of the peregrine falcon was predicted to have a negative PSORT score (−1.41), which suggested that the MTS does not tend to target

3
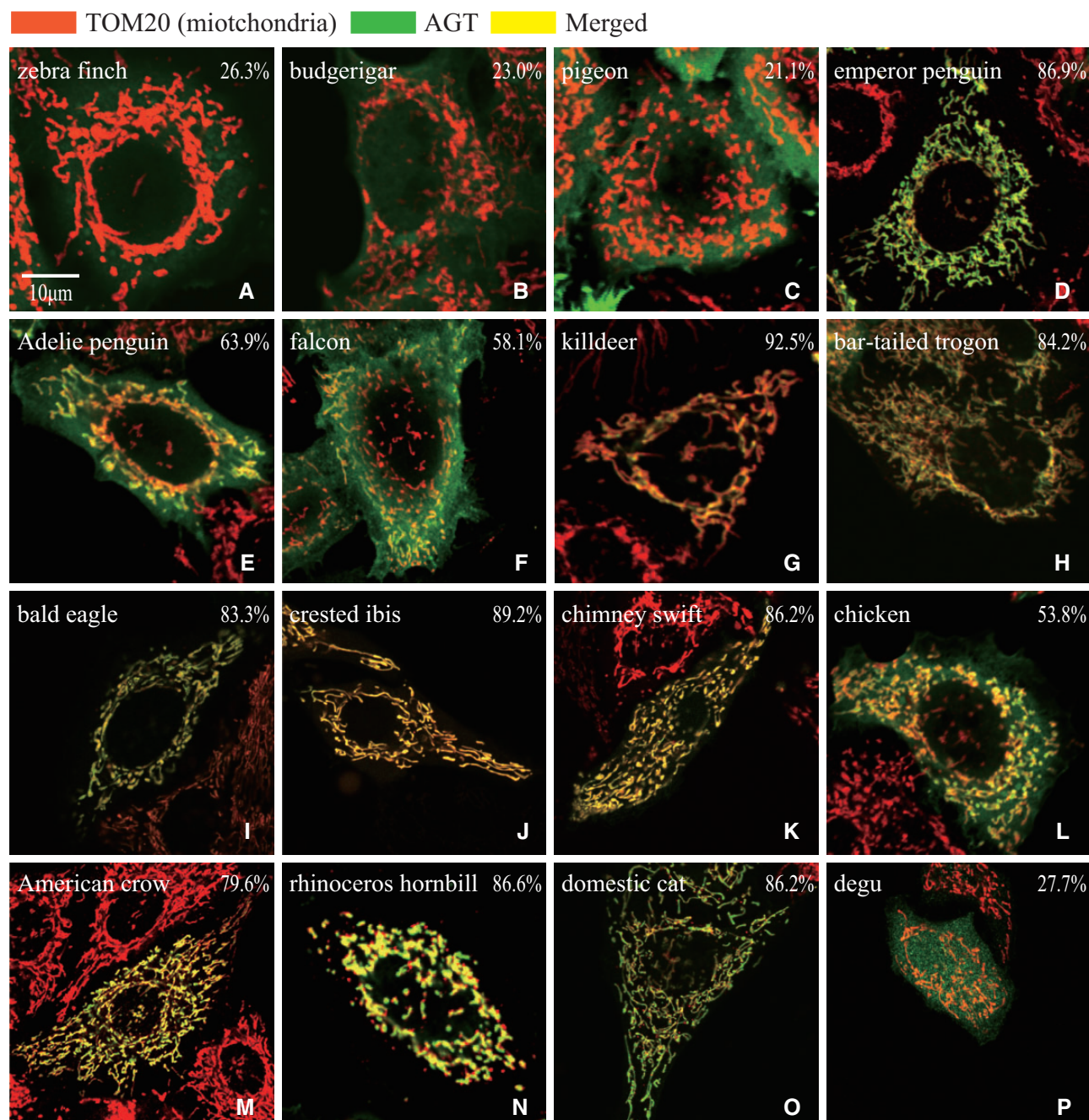
FIG. 3. AGT mitochondrial targeting in different bird species. HeLa cells were transiently transfected with constructs of (*A*) zebra finch, (*B*) budgerigar, (*C*) pigeon, (*D*) emperor penguin, (*E*) Adélie penguin, (*F*) falcon, (*G*) killdeer, (*H*) bar-tailed trogon, (*I*) bald eagle, (*J*) crested ibis, (*K*) chimney swift, (*L*) chicken, (*M*) American crow, (*N*) rhinoceros hornbill, (*O*) domestic cat, and (*P*) degu. AGT and mitochondria are labeled in green and red, respectively; colocalization of green and red fluorescence signals is indicated by a yellow fluorescence (Merged). The mitochondrial targeting efficiency of AGT for each species is shown in the upper right corner of each panel. Magnification is the same for all panels.

mitochondria; in fact, this species is an obligate carnivore (100% meat in its diet; supplementary table S4, Supplementary Material online). This finding indicates either a low accuracy of PSORT prediction, or no correlation between diet and AGT targeting in birds.

To directly measure the AGT mitochondrial targeting efficiency in birds, we next conducted an improved cell-based functional assay that was developed previously (Birdsey et al. 2004). Plasmid constructs containing the MTS and mature region of AGT from each bird were attached to the

N-terminus of FLAG-tag, and transiently expressed in the HeLa cells. Mitochondrial targeting efficiencies of the constructs were determined by confocal fluorescence microscopy (see Materials and Methods for experimental details; fig. 3). Unlike the previous study (Birdsey et al. 2004), in which only the MTS (excluding the mature region) of AGT was fused to the green fluorescent protein (GFP) in plasmid constructs, here we made plasmid constructs with the full-length coding region of AGT-including both the MTS and mature regions. This was because nonsignal peptide regions can also impact
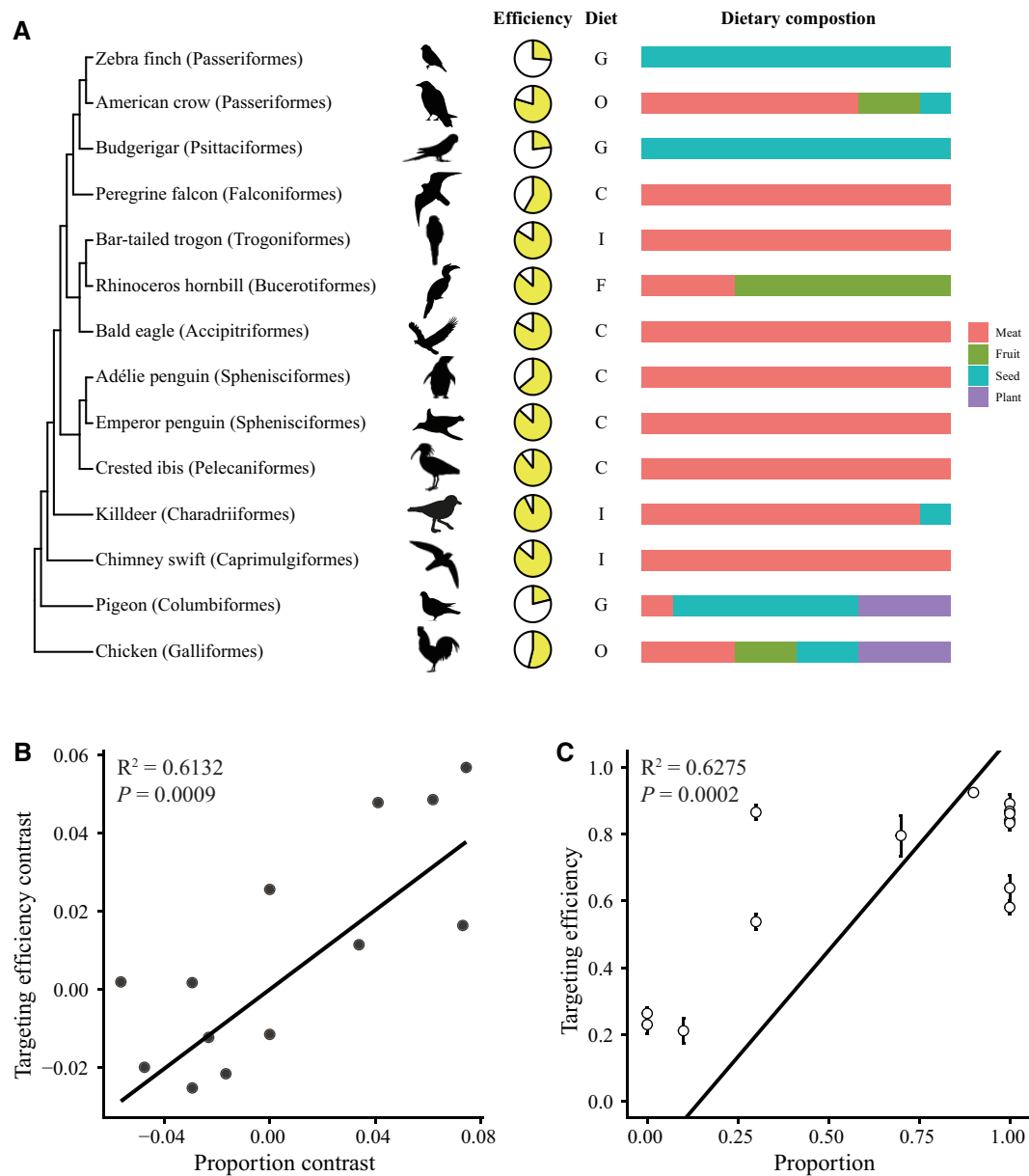
FIG. 4. Positive correlation between mitochondrial targeting efficiencies of AGT and proportions of animal tissue in avian diet. (A) Mitochondrial targeting efficiencies and dietary compositions for 14 bird species. Targeting efficiency for each species is depicted in a pie chart. The dietary compositions were taken from the EltonTraits 1.0 database and are shown by bar graphs. (B) Positive correlation between phylogenetically independent contrast (PIC) in mitochondrial targeting efficiency and proportion of animal tissue in diet. (C) PGLS regression of the mitochondrial targeting efficiency versus the proportion of diet consisting of animal tissue. Silhouettes were taken from phylopic.org.

the subcellular localization of an enzyme (Purdue et al. 1990; Motley et al. 1995; Zhang et al. 2003). As a full-length AGT was successfully identified in 14 avian genomes, a total of 14 plasmids were constructed (supplementary table S1, Supplementary Material online). AGT genes of the 14 birds were all successfully expressed in cells, hence AGT mitochondrial targeting efficiencies were directly measured in all 14 birds (figs. 3 and 4, supplementary table S5, Supplementary Material online). The mitochondrial targeting efficiency of AGT in each bird varied from 21.1% in the pigeon to 92.5% in the killdeer (fig. 3). Notably, the levels of mitochondrial targeting in three unrelated granivores (zebra finch, budgerigar, and pigeon) have been greatly diminished independently

(from 21.1% to 26.3%; figs. 3A–C and 4A), suggesting that AGT tends to target peroxisomes rather than mitochondria in herbivorous birds. In contrast, insectivores and carnivores often generated a higher level of mitochondrial targeting (from 63.9% to 92.5%), as shown by the colocalization of AGT with the mitochondrial outer membrane protein TOM20 (yellow color in figs. 3D–K and 4A). This suggests that AGT tends to target mitochondria in insectivorous or carnivorous birds. The amount of AGT and mitochondria colocalization in an image was calculated automatically by a statistical approach that avoids visual interpretation bias (see Materials and Methods). Serving as positive controls, the measured AGT in the three carnivorous mammals had

a high level of mitochondrial targeting efficiency (86.2% in cat, 95.0% in hedgehog, and 92.1% in dog; fig. 3O, supplementary fig. S2A and B, Supplementary Material online, and supplementary table S6, Supplementary Material online). Consistently, this subcellular targeting was previously detected to be mostly mitochondrial, based on immunoelectron microscopic observations and cell-based assays (Lumb et al. 1994; Birdsey et al. 2004). In contrast, the negative controls (three known herbivorous mammals) showed a low level of AGT mitochondrial targeting efficiency (27.7% in degu, 18.2% in Sumatran orangutan, and 20.2% in rhesus monkey; fig. 3P, supplementary fig. S2C and D, Supplementary Material online, and supplementary table S6, Supplementary Material online), an observation that is consistent with peroxisomal targeting of AGT in the same species examined by immunoelectron microscopy (Birdsey et al. 2005). We additionally synthesized AGT sequences of the two birds (Anna's hummingbird and cuckoo roller) without an intact MTS (fig. 2), serving as negative controls, and determined their mitochondrial targeting efficiencies using the same approach. As expected, AGTs of these two birds cannot target mitochondria efficiently (supplementary fig. S3, Supplementary Material online).

Fluctuation in the mitochondrial targeting efficiency of AGT was observed in avian species (fig. 3). However, it remains untested whether AGT subcellular distribution is significantly correlated with natural diets across birds. To test whether diet is associated with mitochondrial targeting efficiency of AGT in birds, we carried out two comparative analyses, both of which can circumvent the nonindependence of traits and minimize problems associated with phylogenetic inertia. First, we conducted a phylogenetically independent contrast (PIC) analysis (Felsenstein 1985). The experimentally determined AGT mitochondrial targeting efficiencies and proportions of animal tissue in the diet were converted into separate PICs, and a regression analysis was applied. We observed a significant positive correlation between the PICs of mitochondrial targeting efficiencies and those of proportions of animal tissue in the diet ($R^2 = 0.6132$, $P = 0.0009$; fig.4B). Second, we conducted a phylogenetic generalized least squares (PGLS) regression analysis (Grafen 1989). We observed a positive relationship between mitochondrial targeting efficiencies and proportions of animal tissue in the diet ($R^2 = 0.6275$, $P = 0.0002$; fig.4C). In contrast, we did not observe a significant correlation between PSORT scores and diet in birds (supplementary fig. S4, Supplementary Material online), although the correlation was significant in mammals (Birdsey et al. 2004; Liu et al. 2012).

Thus, there appears to be a trend toward increasing mitochondrial targeting efficiencies of AGT in birds as proportions of animal tissue in the diet increase (fig. 4). This suggests that variable efficiencies of AGT mitochondrial targeting in birds may be an adaptive characteristic driven by dietary selection pressure. Notably, mismatches were observed between computationally predicted PSORT scores and experimentally determined targeting efficiencies (supplementary table S4, Supplementary Material online). This suggests that caution must be taken when using only computer prediction to understand the evolution of protein subcellular targeting.

In contrast to highly variable targeting efficiencies to mitochondria, AGTs in different birds may have high efficiencies of peroxisomal targeting that are comparable to one another, due to the conserved C-terminal PTS1. To investigate the peroxisomal targeting efficiency of AGT in different birds, we additionally fused the FLAG tag to the N-terminus of mature region of 10 birds (supplementary fig. S5, Supplementary Material online). Regardless of their diets, AGTs of all these 10 birds were localized to the peroxisome with a high efficiency (from 78.8% to 85%; supplementary fig. S5, Supplementary Material online and supplementary table S7, Supplementary Material online). These results supported our inference that avian AGTs have similar and high efficiencies of peroxisomal targeting due to the conserved C-terminal PTS1. We also examined previously reported species as positive (human) and negative (African clawed frog) controls (Noguchi and Takada 1978, 1979; Holbrook and Danpure 2002). The peroxisomal located human AGT showed a high targeting efficiency comparable to birds (78.5%), and the *Xenopus* AGT, which has been reported to be mitochondrial and cytosolic (Holbrook and Danpure 2002), cannot target to peroxisomes in our experiments (3.3%; supplementary fig. S5, Supplementary Material online and supplementary table S7, Supplementary Material online).

Detecting Molecular Adaptation to Avian Diet

Molecular adaptation is typically identified by the presence of positive selection, which is characterized by an elevated ratio of nonsynonymous to synonymous substitution rate ($d_N/d_S > 1$, or $\omega > 1$). Given the diet-related variation of mitochondrial targeting efficiency of AGT in birds, we attempted to test whether positive selection has acted on the *AGT* gene, especially on the MTS region which has a direct role in determining the mitochondrial targeting efficiency of AGT.

We first estimated the nonsynonymous substitution rate (d_N), synonymous substitution rate (d_S), and the ratio of d_N/d_S (ω) using a likelihood method (Yang 2007). In the data set of 21 species, which included the 14 bird species with full-length *AGTs* and seven reptile species, we examined a model in which each branch has an independent ω (see model A and data set I in supplementary table S8, Supplementary Material online). We next plotted d_N against d_S values (fig. 5A), both of which were generated from model A (supplementary table S8, Supplementary Material online). In the MTS region of AGT, 11 of the 26 branches connecting birds displayed d_N values that were higher than d_S ($d_N > d_S$; fig. 5A), which is a signature of positive selection ($\omega > 1$). In contrast, in the mature region of AGT, only two of the 26 branches showed $d_N > d_S$ (fig. 5A). Furthermore, we calculated pairwise estimates of d_N and d_S values, using both the modified Nei-Gojobori (Zhang et al. 1998) and maximum-likelihood (Goldman and Yang 1994) methods. Similar to the results of our predictive model, both methods indicated that 49.45% and 74.73%, respectively, of the pairwise comparisons had $d_N > d_S$ in the MTS region. However, no cases of $d_N > d_S$ were detected in the mature region (fig. 5B and C). Thus,
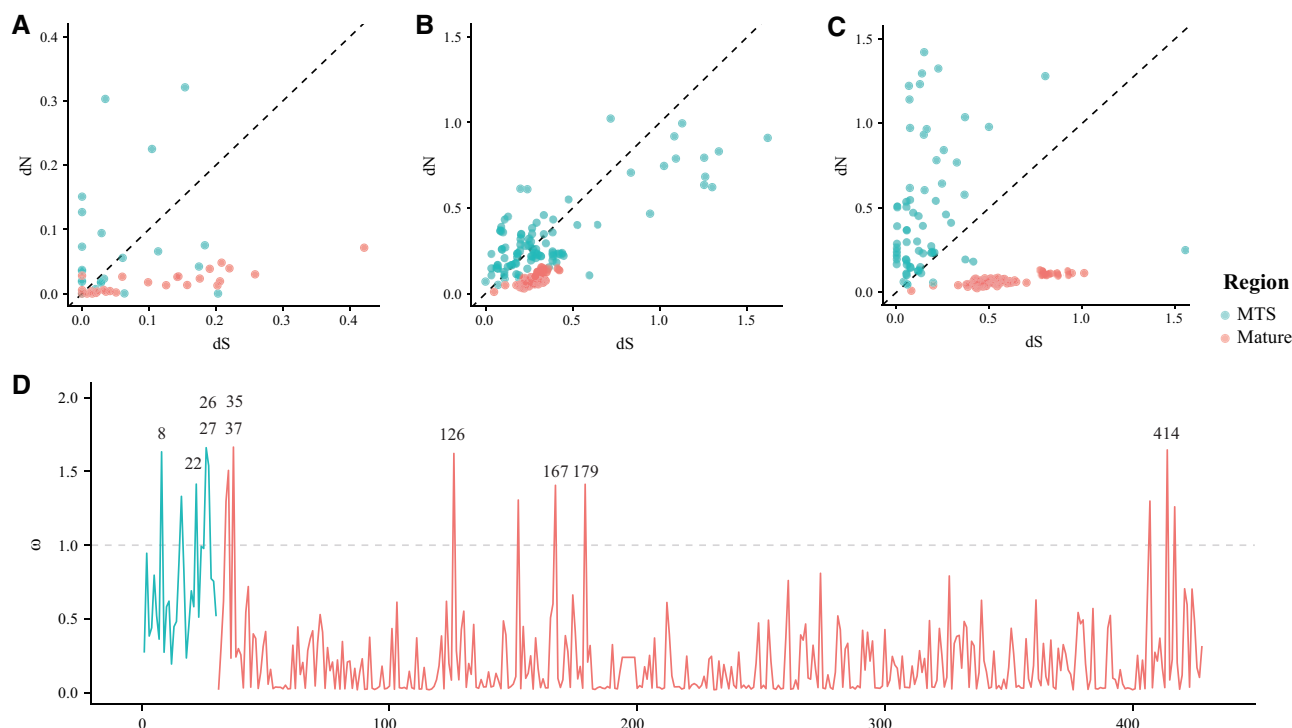
FIG. 5. Contrasting modes of evolution between the MTS and mature regions of *AGT* in birds. The synonymous (d_S) and nonsynonymous (d_N) substitution rates estimated from (A) the free-ratio model, (B) modified Nei-Gojobori method, (C) pairwise maximum-likelihood approach, and (D) M8 site model.

these findings indicate that the MTS region of AGT has undergone positive selection, whereas the mature region has been under purifying selection. This indication was further supported by our subsequent analyses. In the data set consisting of the AGT mature regions from the 14 birds with full-length *AGT*s, we assumed a uniform ω for all lineages (see data set II and model H in supplementary table S8, Supplementary Material online). According to this model, ω was estimated to be 0.132, which is significantly smaller than 1 ($P = 1.38 \times 10^{-200}$; supplementary table S8, Supplementary Material online). Similar results were obtained after examining two other data sets containing AGT mature regions (Data Sets I and III, supplementary table S8, Supplementary Material online). These results reinforce our findings (described above) that the mature regions of AGT have been under strong purifying selection in birds. In contrast, when similarly assuming a uniform ω in the MTS region of all lineages (see data set IV and model N in supplementary table S8, Supplementary Material online), ω was estimated to be 2.204, which is significantly >1 ($P = 0.039$; supplementary table S8, Supplementary Material online). These findings provide further support that the MTS regions of AGT have undergone positive selection in birds.

To test whether any codon positions of AGT have been subjected to positive selection, a pair of models (M8 and M8a) were compared (Swanson et al. 2003). M8 assumes a beta distribution for ω among sites with $0 < \omega < 1$, and allows an extra class of sites to have $\omega > 1$; M8a is same to M8, but allows the extra class of sites to have $\omega = 1$ (Yang 2007). In a data set consisting of 14 bird and seven reptile

species, model M8 was significantly better than its null model M8a ($P = 8.7 \times 10^{-4}$; supplementary table S8, Supplementary Material online), suggesting that a proportion of codons have undergone positive selection. The model M8 detected four and six codons that are potentially under positive selection in the MTS and mature regions, respectively (fig. 5C and supplementary table S8, Supplementary Material online). Given that the MTS region contains 30 codons and the mature region has 398 in the sequence alignment, the proportion of sites under putative positive selection is significantly greater for the MTS region (4/30 = 13.3%) than for the mature region (6/398 = 1.5%; $P < 0.005$, Fisher's exact test). In three other data sets containing only the MTS regions (Data Sets IV–VI, supplementary table S8, Supplementary Material online), model M8 was always significantly better than model M8a, and several codons were detected to be sites under putative positive selection (supplementary table S8, Supplementary Material online). These results also suggest that the MTS regions of AGT may have been subjected to positive selection in birds.

We observed a shift in selective pressure between the ancestral lineage leading to all of the 14 bird species examined (i.e., common ancestral lineage) and all other avian lineages. In data set I, which consisted of full-length *AGT* genes of the 14 bird and seven reptile species, we examined a model that allows ω to vary between the common ancestral lineage (i.e., the common ancestor of all examined birds) and all other bird lineages (model D, supplementary table S8, Supplementary Material online). This was then compared with a simpler model that assumes a uniform ω for all bird

lineages (model E, supplementary table S8, Supplementary Material online), which yielded a significant difference ($P = 3.852 \times 10^{-7}$). This finding suggests that the common ancestor of all examined birds (i.e., common ancestral lineage) has a significantly smaller ω than all other bird lineages (0.045 vs. 0.174, supplementary table S8, Supplementary Material online). A similar result was obtained with another data set that includes only AGT mature regions (see models L and M in data set III, supplementary table S8, Supplementary Material online). Thus, AGTs in birds have undergone even stronger purifying selection in the common ancestor of all examined birds than in all other bird lineages.

Discussion

In this study, we characterized the evolution of the liver enzyme AGT in taxa that represent most major lineages of birds. Using an improved cell-based functional assay, we identified a significant positive correlation between the mitochondrial targeting efficiency of AGT and the proportion of animal tissue in diet; however, this correlation was not observed when using computationally predicted AGT targeting. Several analytical approaches consistently detected signatures of molecular adaptation in the MTSs of AGT that were not found in corresponding mature regions.

Birds, like mammals, appear to have a clear link between AGT targeting and diet. For example, mitochondrial targeting efficiencies in granivores have been independently diminished (fig. 3A–C), which is consistent with the absence of animal tissue in the diet of these seed-eating birds. Furthermore, we find variability in AGT mitochondrial targeting efficiency among birds (fig. 3), and demonstrate a significant positive correlation between avian carnivorous diet and AGT mitochondrial targeting efficiency (fig. 4B and C). However, a notable discordance was observed in two particular species. Specifically, according to the positive correlation between AGT mitochondrial targeting efficiencies and proportion of animal tissue in the diet, the rhinoceros hornbill, a frugivorous bird, should mainly target peroxisomes. According to our cell-based assay, however, this bird appeared to have a mitochondrial AGT, with a mitochondrial targeting efficiency of 86.6% (fig. 3N). Although the rhinoceros hornbill is considered a frugivorous species, it does feed on a substantial amount of animal tissue (~30% in its diet; fig. 4A and supplementary table S9, Supplementary Material online) and/or a relatively small amount of glycolate in ripe fruits (2–3 mg/100g wet weight; Harris and Richardson 1980). Common wild fruits provide birds with mostly simple carbohydrates or fats, but relatively little protein (Witmer 1998; Smith et al. 2007). Thus, it is critical for frugivores to consume sufficient animal proteins beyond fruits in order to fulfill their nitrogen requirements (Izhaki and Safriel 1989; Izhaki 1992). This may cause strong purifying selection for maintaining a functional MTS in the rhinoceros hornbill. Another discordance was detected in an insectivorous bird, the cuckoo-roller, although this case is more difficult to explain. We detected a missense mutation in the upstream translation start site (fig. 2), suggesting that the MTS is nonfunctional and thus mitochondrial targeting has

been lost. However, 70% of this bird diet consists of invertebrates and 30% is ectothermic vertebrates (Wilman et al. 2014). Hence, AGT of this bird was expected to mainly target mitochondria, following the correlation between diet and AGT targeting. As a result, the compensatory mechanism for the cuckoo-roller to detoxify glyoxylate remains unknown. Certainly, in addition to diet, other factors such as alternative locations of glyoxylate formation may also affect the evolution of AGT, which should be examined when such data become available in future. Moreover, the feeding habits of most animals are not so clear-cut. In many instances, species are assigned to different categories of food habits using the food type predominated in the stomachs of 51% or more (Wilson 1974; Wang and Zhao 2015). This method classifies different species into very few categories, which may overlook the highly dynamic and diverse food compositions in different species. Thus, such complexity of food composition would lead to bias in predicting the relationship between diets and AGT subcellular targeting. It should be noted that, while avian AGT evolution clearly shows how dietary changes are correlated with molecular evolution, other similar examples such as taste receptors (Baldwin et al. 2014; Hong and Zhao 2014), ribonucleases (Zhang et al. 2002), amylases (Perry et al. 2007; Pajic et al. 2019), chitinases (Emerling et al. 2018), and trehalase (Jiao et al. 2019) may have also played an important role in driving molecular adaptation in relation to avian diet evolution.

Unlike mammals, which show a number of repeated losses of MTS (Liu et al. 2012), only two bird species—the Anna's hummingbird and cuckoo-roller—had a nonfunctional MTS with missense mutations in the upstream translation start site (fig. 2). It is logical that the hummingbird does not have a mitochondrial AGT, since 90% of their diet is composed of nectar (Wilman et al. 2014). We also identified missense mutations in the upstream translational site in three passerine birds (zebra finch, medium ground finch, and American crow), but an alternative translation start site was identified 15-bp downstream in each bird (fig. 2). This alternative translation start site appeared to be functional, as demonstrated by the cell-based assay (fig. 3A and M), although the assay did not include the medium ground finch because a full-length AGT was not identified in this bird (supplementary table S1, Supplementary Material online). Thus, these results suggest that alternative translation start sites cannot be ignored when attempting to understand diet and the evolution of enzyme targeting, as has been done elsewhere (Zhang et al. 2014).

Unlike other vertebrates, all birds in this study were found to have highly conserved PTS1 sequences (supplementary fig. S1, Supplementary Material online), which matched the PTS1 consensus sequence (Gould et al. 1989; Swinkels et al. 1992). The consensus PTS1 is sufficient to direct the peroxisomal targeting of a wide range of proteins, including AGT, without the need of any ancillary targeting sequences (Gould et al. 1989; Swinkels et al. 1992; Holbrook and Danpure 2002). In contrast, PTS1 sequences that do not match the consensus sequence (for instance, KKL in human AGT) require ancillary peroxisomal targeting other than C-terminal tripeptide (Motley et al. 1995; Oatey, Lumb, Jennings, et al. 1996).

Indeed, the peroxisomal targeting of AGT has been observed in a bird species by immunoelectron microscopy (Danpure et al. 1994). It appears that the most parsimonious inference is that some level of peroxisomal targeting for AGT may be required in the common ancestor of birds. Consistent with this inference, we detected a signature of stronger purifying selection and functional constraint on AGT in the common ancestral lineage of all examined birds (supplementary table S8, Supplementary Material online), indicating that some level of AGT peroxisomal targeting and a herbivorous diet may be important in ancestral birds. Indeed, ancestral state reconstructions using dietary preferences of extant birds indicated that the common ancestor of Neornithes (i.e., modern birds) was most likely granivorous to some extent (Larson et al. 2016; Chen and Zhao 2019). The evolution of granivory and associated toothless beak were assumed to play a key role in the survival of Neornithes at the end-Cretaceous mass extinction (Larson et al. 2016). It is worth mentioning that our experiment revealed convergent reduction of AGT mitochondrial targeting efficiencies in all granivores tested here (figs. 3A–C and 4A), suggesting that peroxisomal detoxification of AGT plays an important role for seed-eating birds.

Previous studies have shown that decreases of AGT mitochondrial targeting in Primates and Carnivora have been driven by positive selection (Holbrook et al. 2000; Birdsey et al. 2004). Similarly, our study also revealed molecular signatures of positive selection on avian MTSs, although the evolution of the mature regions of AGT has been shaped predominately by purifying selection (fig. 5). Furthermore, we also observed decreases of AGT mitochondrial targeting in three unrelated granivorous birds (fig. 4A), although these species still have a complete and functional MTS. We hypothesized that the preservation of mitochondrial targeting in birds may have resulted from strong selective pressure to meet protein and amino acid requirements, especially during their breeding season. Moreover, mitochondrial targeting of AGT may have been favored by granivores when transitioning to other dietary niches, as shown by the high transition rate from granivores to omnivores in birds (Burin et al. 2016). Somewhat surprisingly, mitochondrial targeting of AGT in some specialists has been fully abolished by the loss of MTS, as was seen in the Anna's hummingbird (fig. 2). According to Dollo's law (Dollo 1893), it is unlikely for these specialists to regain a functional MTS by accumulation of random mutations, thus preventing the transition of specialists to different dietary niches. Specialists usually develop a wide range of adaptations specific to a particular food or foraging substrate (Birdsey et al. 2004; Abrahamczyk and Kessler 2015), which may make them more vulnerable when their preferred food resources become less available (Wilson and Yoshimura 1994). For instance, the loss of functional MTS can help the AGT of Anna's hummingbird target peroxisomes more effectively, which may be helpful for glyoxylate detoxification after nectar consumption. However, it may prevent the hummingbird species from feeding on other food resources such as vertebrates, due to its inability to detoxify animal-derived glyoxylate. Human-induced global change has reduced the availability and predictability of many food resources, and this challenge will become more obvious for some specialists in the future (Burin et al. 2016).

Although computationally predicted mitochondrial targeting efficiencies of AGT were largely correlated with diet in mammals (Liu et al. 2012), our study showed a number of mismatches between computationally predicted and experimentally determined AGT targeting efficiencies in birds (supplementary table S4, Supplementary Material online). We detected a positive correlation between avian diets and experimentally determined AGT targeting (fig. 4), but no such relationship was detected when using computationally predicted AGT targeting (supplementary fig. S4, Supplementary Material online). These disparities may have resulted from biases of computer prediction, which suggests that our current understanding of protein subcellular localization is limited (Nakai and Horton 1999). Even in the model organisms with abundant experimental data, such as yeast, the overall predictive accuracy of PSORT can only reach to 57% (Nakai and Horton 1999). We speculate that the biases of PSORT prediction may have resulted from its small training data set, overrepresentation of mammals in its data set, and consideration of first 20 amino acids of MTS while birds having a longer MTS (23–30 amino acids) than mammals (22 amino acids; Vonheijne et al. 1989; Nakai and Horton 1999). Despite that the PSORT computer prediction in mammals is generally consistent with experimental data based on immunoelectron microscopy and cell-based assays (Birdsey et al. 2004; Birdsey et al. 2005; Liu et al. 2012), some species without experimental data do not have consistent patterns between computer prediction and their natural diets. For instance, the PSORT score of an obligate insect-eating bat *Miniopterus fuliginosus* (−0.31) was predicted to be even smaller than that of an obligate fruit-eating bat *Pteropus vampyrus* (−0.17; Liu et al. 2012). This mismatch implies that there are significant biases and/or inaccuracies when using computational prediction to determine the AGT subcellular distribution, and suggests that experimental data are superior and should be considered accordingly.

Overall, this study identified signatures of molecular adaptation of a dietary enzyme AGT, and found that diet may have affected the evolution of AGT subcellular targeting in birds. Consequently, these results contribute to our understanding of how diet drives molecular adaptations, and also highlight the caveat of using computationally predicted protein subcellular targeting.

Materials and Methods

Genome Data

Genome assemblies of the 48 birds were obtained from the Avian Phylogenomics Project (http://avian.genomics.cn/en/, last accessed January 1, 2016). Genome assemblies of one lizard (*Gekko japonicus*), one snake (*Ophiophagus hannah*), two turtles (*Chrysemys picta*, *Chelonia mydas*), two alligators (*Alligator sinensis*, *Alligator mississippiensis*), and one crocodile (*Crocodylus porosus*) were downloaded from the National Center for Biotechnology Information (NCBI) database (https://www.ncbi.nlm.nih.gov/; last accessed December 15,

2017) and used as outgroups (Green et al. 2014). See supplementary table S2, Supplementary Material online for further details of the genome assemblies used in this study.

Gene Identification

The gene encoding AGT contains an N-terminal MTS and a C-terminal PTS1 (Motley et al. 1995; fig. 1B). We conducted TBLASTN (v2.7.1) (Altschul et al. 1990) to search against the genome assemblies of the chicken *Gallus gallus* and zebra finch *Taeniopygia guttata* using the human AGT protein sequence (NCBI accession number: NM_000030.2) as a query, with a cutoff *e*-value of 1×10^{-10}. Aligned sequences were retrieved from the whole-genome sequences, and exon–intron structures were inferred by GeneWise (Birney et al. 2004). Next, we used full-length AGT protein sequences of the chicken and zebra finch as queries to search against other avian genomes using the same approach. The MTS regions were identified by eye after aligning deduced amino acid sequences of these genes. To investigate the evolution of PTS1 in a phylogenetic framework, we collected all annotated *AGT* genes (also known as *AGXT*) from the genomic assemblies of tetrapods that are available in the UCSC Genome Database (http://genome.ucsc.edu/; last accessed November 15, 2017). The accession numbers of *AGT* genes with available PTS1 sequences are listed in supplementary table S3, Supplementary Material online. The topology of the tetrapod phylogenetic tree was taken from recent studies (Green et al. 2014; Liu et al. 2017).

Diet Composition

We quantified the diet composition of birds based on the EltonTraits 1.0 database (Wilman et al. 2014). This database compiles dietary attributes for a taxonomically wide range of bird and mammal species, including the 20 species (14 birds and six mammals) used in our cell-based experiments. Ten different types of food (invertebrates, endotherms, ectotherms, fishes, unknown vertebrates, carrion, fruits, nectar, seeds, and other plant materials) were defined, and each species was assigned a percentage of each dietary item. Because of the lack of nectar-consuming species in our experiments, the dietary types were collapsed into the following categories: meat, fruits, seeds, and other plant material. The amount of meat in the diet was defined as the sum of abundance of invertebrates, endotherms, ectotherms, fishes, and carrion. Each species was assigned to the corresponding dietary categories based on the relative abundance of diet components. The categories of PlantSeed, FruiNect, Invertebrate, VertFishScav, and Omnivore in EltonTraits corresponded to granivores, frugivores, insectivores, carnivores, and omnivores, respectively, in the current analysis. The diet compositions and food categories of the 14 birds and six mammals examined in our cell-based assays are listed in supplementary tables S9 and S10, Supplementary Material online.

Molecular Evolutionary Analysis

Deduced amino acid sequences were aligned using the MUSCLE program in MEGA7 (Edgar 2004; Kumar et al. 2016). Estimation of d_N/d_S (ω) among different lineages was performed by the codon-based maximum-likelihood method using the CODEML program in PAML4.9 (Yang 2007). This ω ratio indicates selective pressure at the protein level. Specifically, $\omega < 1$ suggests negative or purifying selection, $\omega = 1$ suggests neutral evolution, and $\omega > 1$ suggests positive selection. Likelihood ratio tests using the chi-square approximation were applied to compare nested models. To examine selection pressure in different regions of the *AGT* gene, we determined the ω ratio for each pairwise species comparison using the modified Nei-Gojobori method and maximum-likelihood method implemented in MEGA7 and PAML4.9, respectively (Goldman and Yang 1994; Zhang et al. 1998).

Owing to the statistical nonindependence of species' characters due to phylogenetic inertia (Felsenstein 1985), we employed two phylogenetic comparative methods to examine the potential impact of diet on AGT mitochondrial targeting efficiency. First, we used a PICs analysis using the R package APE (Paradis et al. 2004). Second, we performed PGLS regression analysis in a maximum-likelihood framework using the program Continuous implemented in BayesTraits V3, while Pagel's λ was estimated simultaneously (Pagel 1997, 1999). The phylogenetic tree and branch lengths used in this phylogenetic comparative analysis were obtained from a previously published avian phylogeny (Jarvis et al. 2014) and the TimeTree database (http://www.timetree.org/; last accessed January 15, 2018). The mitochondrial targeting efficiency of AGT was measured by colocalization as described below.

Plasmid Construction

Codon optimized full-length AGTs that include the MTS and mature regions from different species were synthesized and inserted into the pFLAG-N3 vector. As shown in supplementary fig S6A, Supplementary Material online, each full-length AGT (also referred to as MTS-AGT) cloned into the multiple cloning site in frame was fused to the N-terminus of FLAG-tag, which allowed us to study cellular localization by immunofluorescence with an antibody against the FLAG epitope. The 3×FLAG-tag fused at C-terminus of AGT allowed the subcellular localization of the protein to be studied with an antibody against this peptide conveniently. The native folding and biological activity of AGT protein would not be interfered by FLAG-tag because of the small size and hydrophilic nature of this polypeptide marker (Hopp et al. 1988; Einhauer and Jungbauer 2001). These intrinsic features of our method allow us to determine the subcellular localization of AGT from diverse organisms reliably and easily. To choose positive and negative controls, we used the following criteria: available genome sequences, and consistent data of immunoelectron microscopy and PSORT prediction. We thus selected three species of carnivorous mammals (cat, dog, and hedgehog) and three species of herbivorous mammals (degu, rhesus monkey, and Sumatran orangutan), serving as positive and negative controls, respectively.

To determine the peroxisomal targeting of AGT in different species, the mature region was amplified from the pFLAG-N3 vector using the high-fidelity KOD-Plus-Neo

DNA polymerase (Toyobo, Japan). PCR products were purified and then inserted into the pMSCVpuro vector with the sequence of FLAG tag in the 5′-end of *AGT* gene (supplementary fig. S6B, Supplementary Material online).

Cell Culture and Transfection
HeLa cells were maintained in Dulbecco's Modified Eagle's Medium supplemented with 10% fetal bovine serum, 1% penicillin/streptomycin, and 1% L-glutamine at 37 °C with 5% CO_2. Lipofectamine 2000 and Opti-MEM I (Invitrogen, Carlsbad, CA, USA) were used for transient transfection with expression constructs following the manufacturer's instructions.

Immunostaining
At 36 h post transfection, cells were subsequently fixed with 4% paraformaldehyde for 20 min, washed with PBS buffer three times, and incubated in buffer (PBS and 0.1% Triton X-100) for 10 min. Cells were then blocked with PBS plus 5% FBS buffer at 4 °C overnight.

In the experiments determining mitochondrial targeting efficiencies, cells were incubated with primary antibodies (anti-TOM20 1:800; anti-FLAG 1:500) diluted in PBS plus 5% FBS buffer for 2 h at room temperature (RT). Cells were rinsed with PBS buffer three times. Fluorescent secondary antibody (1:1,000 in PBS) was used to incubate cells for 1 h at RT. Finally, cells were washed three times with PBS, and slides were analyzed using an Olympus confocal microscope (Olympus Corporation, Tokyo, Japan).

In the experiments determining peroxisomal targeting efficiencies, the peroxisomes in the HeLa cell line we used in this study show green fluorescence due to the stable expression of peroxisomal targeted enhanced green fluorescence protein (EGFP). Cells were incubated with anti-FLAG rabbit polyclonal antibody (proteintech, catalog no. 20543-1-AP, 1:400) for 1 h at RT. A Cy3-conjugated goat antirabbit secondary antibody (proteintech, catalog no. SA00009-2, 1:800) was used for 1.5 h at RT for fluorescence visualization. Finally, cells were washed three times with PBS, and slides were analyzed using an Olympus confocal microscope (Olympus Corporation, Tokyo, Japan).

Confocal Microscopy and Image Processing
Confocal microscopy was performed with an Olympus FV1000 confocal laser scanning microscope with an UPLSPO 60× numerical aperture 1.35 oil objective. The FV10-ASW 3.0 software (Olympus Corporation, Tokyo, Japan) was used for image processing and analysis. Colocalization was quantified by the ImageJ plug-in JACoP (Bolte and Cordelieres 2006; Schindelin et al. 2012). We cropped the image to separate each cell, and measured the colocalization for individual cells. The mitochondrial colocalization efficiency of each cell was defined as the fraction of AGT that colocalized with mitochondria, as measured with Mander's Colocalization Coefficients (MCC) with an automatic threshold (Manders et al. 1993; Dunn et al. 2011). Because the targeting efficiency is slightly different among different cells, we are able to obtain values with a range (instead of a single value) for each species. We used the same approach to determine peroxisomal targeting efficiencies.

Supplementary Material
Supplementary data are available at *Molecular Biology and Evolution* online.

Acknowledgments

Author Contributions
H.Z. conceived and designed project. B.J.W. and J.M.X. conducted molecular evolutionary analysis. B.J.W., J.M.X., Q.W., and J.L.Y. performed cell-based assay. Z.S. supervised cell-based assay. H.Z. and B.J.W. wrote the manuscript. All authors have read, edited, and approved the manuscript.

References
Abrahamczyk S, Kessler M. 2015. Morphological and behavioural adaptations to feed on nectar: how feeding ecology determines the diversity and composition of hummingbird assemblages. *J Ornithol*. 156(2):333–347.

Altschul SF, Gish W, Miller W, Myers EW, Lipman DJ. 1990. Basic local alignment search tool. *J Mol Biol*. 215(3):403–410.

Baldwin MW, Toda Y, Nakagita T, O'Connell MJ, Klasing KC, Misaka T, Edwards SV, Liberles SD. 2014. Evolution of sweet taste perception in hummingbirds by transformation of the ancestral umami receptor. *Science* 345(6199):929–933.

Birdsey GM, Danpure CJ. 1998. Evolution of alanine: glyoxylate aminotransferase intracellular targeting: structural and functional analysis of the guinea pig gene. *Biochem J*. 331(1):49–60.

Birdsey GM, Lewin J, Cunningham AA, Bruford MW, Danpure CJ. 2004. Differential enzyme targeting as an evolutionary adaptation to herbivory in carnivora. *Mol Biol Evol*. 21(4):632–646.

Birdsey GM, Lewin J, Holbrook JD, Simpson VR, Cunningham AA, Danpure CJ. 2005. A comparative analysis of the evolutionary relationship between diet and enzyme targeting in bats, marsupials and other mammals. *Proc R Soc B*. 272(1565):833–840.

Birney E, Clamp M, Durbin R. 2004. GeneWise and genomewise. *Genome Res*. 14(5):988–995.

Bolte S, Cordelieres FP. 2006. A guided tour into subcellular colocalization analysis in light microscopy. *J Microsc*. 224(3):213–232.

Burin G, Kissling WD, Guimarães PR, Şekercioğlu ÇH, Quental TB. 2016. Omnivory in birds is a macroevolutionary sink. *Nat Commun*. 7(1):11250.

Chen YH, Zhao H. 2019. Evolution of digestive enzymes and dietary diversification in birds. *PeerJ* 7:e6840.

Cochat P, Rumsby G. 2013. Primary hyperoxaluria. *N Engl J Med*. 369(7):649–658.

Danpure CJ, Cooper PJ, Wise PJ, Jennings PR. 1989. An enzyme trafficking defect in two patients with primary hyperoxaluria type 1: peroxisomal alanine/glyoxylate aminotransferase rerouted to mitochondria. *J Cell Biol*. 108(4):1345–1352.

Danpure CJ, Guttridge KM, Fryer P, Jennings PR, Allsop J, Purdue PE. 1990. Subcellular distribution of hepatic alanine: glyoxylate aminotransferase in various mammalian species. J Cell Sci. 97:669–678.

Danpure CJ, Fryer P, Jennings PR, Allsop J, Griffiths S, Cunningham A. 1994. Evolution of alanine: glyoxylate aminotransferase 1 peroxisomal and mitochondrial targeting. A survey of its subcellular distribution in the livers of various representatives of the classes Mammalia, Aves and Amphibia. Eur J Cell Biol. 64(2):295–313.

Danpure CJ. 1997. Variable peroxisomal and mitochondrial targeting of alanine: glyoxylate aminotransferase in mammalian evolution and disease. Bioessays 19(4):317–326.

Dollo L. 1893. The laws of evolution. Bull Soc Belge Géol Paléontol Hydrol. 7:165–166.

Dunn KW, Kamocka MM, McDonald JH. 2011. A practical guide to evaluating colocalization in biological microscopy. Am J Physiol Cell Physiol. 300(4):C723–C742.

Edgar RC. 2004. MUSCLE: multiple sequence alignment with high accuracy and high throughput. Nucleic Acids Res. 32(5):1792–1797.

Einhauer A, Jungbauer A. 2001. The FLAG (TM) peptide, a versatile fusion tag for the purification of recombinant proteins. J Biochem Biophys Methods. 49(1–3):455–465.

Emerling CA, Delsuc F, Nachman MW. 2018. Chitinase genes (CHIAs) provide genomic footprints of a post-Cretaceous dietary radiation in placental mammals. Sci Adv. 4(5):eaar6478.

Felsenstein J. 1985. Phylogenies and the comparative method. Am Nat. 125(1):1–15.

Gill F, Donsker D. 2013. IOC world bird list (version 3.3). International Ornithologists' Union.

Goldman N, Yang Z. 1994. A codon-based model of nucleotide substitution for protein-coding DNA sequences. Mol Biol Evol. 11(5):725–736.

Gould SJ, Keller GA, Hosken N, Wilkinson J, Subramani S. 1989. A conserved tripeptide sorts proteins to peroxisomes. J Cell Biol. 108(5):1657–1664.

Grafen A. 1989. The phylogenetic regression. Philos Trans R Soc Lond B Biol Sci. 326(1233):119–157.

Grant PR. 1999. Ecology and evolution of Darwin's finches. Princeton, NJ: Princeton University Press.

Green RE, Braun EL, Armstrong J, Earl D, Nguyen N, Hickey G, Vandewege MW, St. John JA, Capella-Gutierrez S, Castoe TA, et al. 2014. Three crocodilian genomes reveal ancestral patterns of evolution among archosaurs. Science 346(6215):1254449.

Harris KS, Richardson KE. 1980. Glycolate in the diet and its conversion to urinary oxalate in the rat. Investig Urol. 18(2):106–109.

Holbrook JD, Birdsey GM, Yang Z, Bruford MW, Danpure CJ. 2000. Molecular adaptation of alanine: glyoxylate aminotransferase targeting in primates. Mol Biol Evol. 17(3):387–400.

Holbrook JD, Danpure CJ. 2002. Molecular basis for the dual mitochondrial and cytosolic localization of Alanine: glyoxylate aminotransferase in amphibian liver cells. J Biol Chem. 277(3):2336–2344.

Hong W, Zhao H. 2014. Vampire bats exhibit evolutionary reduction of bitter taste receptor genes common to other bats. Proc R Soc B. 281(1788):20141079.

Hopp TP, Prickett KS, Price VL, Libby RT, March CJ, Cerretti DP, Urdal DL, Conlon PJ. 1988. A short polypeptide marker sequence useful for recombinant protein identification and purification. Nat Biotechnol. 6(10):1204–1210.

Ichiyama A. 2011. Studies on a unique organelle localization of a liver enzyme, serine: pyruvate (or alanine: glyoxylate) aminotransferase. Proc Jpn Acad Ser B. 87(5):274–286.

Izhaki I, Safriel UN. 1989. Why are there so few exclusively frugivorous birds – experiments on fruit digestibility. Oikos 54(1):23–32.

Izhaki I. 1992. A comparative analysis of the nutritional quality of mixed and exclusive fruit diets for yellow-vented bulbuls. Condor 94(4):912–923.

Jarvis ED, Mirarab S, Aberer AJ, Li B, Houde P, Li C, Ho SYW, Faircloth BC, Nabholz B, Howard JT, et al. 2014. Whole-genome analyses resolve early branches in the tree of life of modern birds. Science 346(6215):1320–1331.

Jiao H, Zhang L, Xie HW, Simmons NB, Liu H, Zhao H. 2019. Trehalase gene as a molecular signature of dietary diversification in mammals. Mol Biol Evol. 36(10):2171–2183.

Kumar S, Stecher G, Tamura K. 2016. MEGA7: molecular evolutionary genetics analysis version 7.0 for bigger datasets. Mol Biol Evol. 33(7):1870–1874.

Larson DW, Brown CM, Evans DC. 2016. Dental disparity and ecological stability in bird-like dinosaurs prior to the end-Cretaceous mass extinction. Curr Biol. 26(10):1325–1333.

Liu L, Zhang J, Rheindt FE, Lei F, Qu Y, Wang Y, Zhang Y, Sullivan C, Nie W, Wang J, et al. 2017. Genomic evidence reveals a radiation of placental mammals uninterrupted by the KPg boundary. Proc Natl Acad Sci U S A. 114(35):E7282–E7290.

Liu Y, Xu H, Yuan X, Rossiter SJ, Zhang S. 2012. Multiple adaptive losses of alanine-glyoxylate aminotransferase mitochondrial targeting in fruit-eating bats. Mol Biol Evol. 29(6):1507–1511.

Lovette IJ, Fitzpatrick JW. 2016. Handbook of bird biology. Hoboken, NJ: John Wiley & Sons.

Lowry M, Hall DE, Brosnan JT. 1985. Hydroxyproline metabolism by the rat kidney: distribution of renal enzymes of hydroxyproline catabolism and renal conversion of hydroxyproline to glycine and serine. Metabolism 34(10):955–961.

Lumb MJ, Purdue PE, Danpure CJ. 1994. Molecular evolution of alanine/glyoxylate aminotransferase 1 intracellular targeting. Analysis of the feline gene. Eur J Biochem. 221(1):53–62.

Maitra U, Dekker EE. 1964. Purification and properties of rat liver 2-keto-4-hydroxyglutarate aldolase. J Biol Chem. 239:1485–1491.

Manders EMM, Verbeek FJ, Aten JA. 1993. Measurement of colocalization of objects in dual-color confocal images. J Microsc. 169(3):375–382.

Marcotte EM, Xenarios I, van der Bliek AM, Eisenberg D. 2000. Localizing proteins in the cell from their phylogenetic profiles. Proc Natl Acad Sci U S A. 97(22):12115–12120.

Motley A, Lumb MJ, Oatey PB, Jennings PR, De Zoysa PA, Wanders RJ, Tabak HF, Danpure CJ. 1995. Mammalian alanine/glyoxylate aminotransferase 1 is imported into peroxisomes via the PTS1 translocation pathway. Increased degeneracy and context specificity of the mammalian PTS1 motif and implications for the peroxisome-to-mitochondrion mistargeting of AGT in primary hyperoxaluria type 1. J Cell Biol. 131:95–109.

Nakai K, Horton P. 1999. PSORT: a program for detecting sorting signals in proteins and predicting their subcellular localization. Trends Biochem Sci. 24(1):34–35.

Neuman RE, Logan MA. 1950. The determination of hydroxyproline. J Biol Chem. 184(1):299–306.

Noguchi T, Takada Y. 1978. Peroxisomal localization of serine: pyruvate aminotransferase in human liver. J Biol Chem. 253(21):7598–7600.

Noguchi T, Takada Y. 1979. Peroxisomal localization of alanine: glyoxylate aminotransferase in human liver. Arch Biochem Biophys. 196(2):645–647.

O'Donnell S, Logan CJ, Clayton NS. 2012. Specializations of birds that attend army ant raids: an ecological approach to cognitive and behavioral studies. Behav Process. 91:267–274.

Oatey PB, Lumb MJ, Danpure CJ. 1996. Molecular basis of the variable mitochondrial and peroxisomal localisation of alanine-glyoxylate aminotransferase. Eur J Biochem. 241(2):374–385.

Oatey PB, Lumb MJ, Jennings PR, Danpure CJ. 1996. Context dependency of the PTS1 motif in human alanine: glyoxylate aminotransferase 1. Ann NY Acad Sci. 804(1): 652–653.

Oda T, Miyajima H, Suzuki Y, Ichiyama A. 1987. Nucleotide sequence of the cDNA encoding the precursor for mitochondrial serine: pyruvate aminotransferase of rat liver. Eur J Biochem. 168(3):537–542.

Olsen AM. 2017. Feeding ecology is the primary driver of beak shape diversification in waterfowl. Funct Ecol. 31(10):1985–1995.

Pagel M. 1997. Inferring evolutionary processes from phylogenies. Zool Scr. 26(4):331–348.

Pagel M. 1999. Inferring the historical patterns of biological evolution. Nature 401(6756):877–884.

Pajic P, Pavlidis P, Dean K, Neznanova L, Romano RA, Garneau D, Daugherity E, Globig A, Ruhl S, Gokcumen O. 2019. Independent amylase gene copy number bursts correlate with dietary preferences in mammals. *Elife* 8:e44628.

Paradis E, Claude J, Strimmer K. 2004. APE: analyses of phylogenetics and evolution in R language. *Bioinformatics* 20(2):289–290.

Perry GH, Dominy NJ, Claw KG, Lee AS, Fiegler H, Redon R, Werner J, Villanea FA, Mountain JL, Misra R, et al. 2007. Diet and the evolution of human amylase gene copy number variation. *Nat Genet*. 39(10):1256–1260.

Purdue PE, Takada Y, Danpure CJ. 1990. Identification of mutations associated with peroxisome-to-mitochondrion mistargeting of alanine/glyoxylate aminotransferase in primary hyperoxaluria type 1. *J Cell Biol*. 111(6):2341–2351.

Schindelin J, Arganda-Carreras I, Frise E, Kaynig V, Longair M, Pietzsch T, Preibisch S, Rueden C, Saalfeld S, Schmid B, et al. 2012. Fiji: an opensource platform for biological-image analysis. *Nat Methods*. 9(7):676–682.

Smith SB, McPherson KH, Backer JM, Pierce BJ, Podlesak DW, McWilliams SR. 2007. Fruit quality and consumption by songbirds during autumn migration. *Wilson J Ornithol*. 119(3):419–428.

Swanson WJ, Nielsen R, Yang Q. 2003. Pervasive adaptive evolution in mammalian fertilization proteins. *Mol Biol Evol*. 20(1):18–20.

Swinkels BW, Gould SJ, Subramani S. 1992. Targeting efficiencies of various permutations of the consensus C-terminal tripeptide peroxisomal targeting signal. *FEBS Lett*. 305(2):133–136.

Takayama T, Fujita K, Suzuki K, Sakaguchi M, Fujie M, Nagai E, Watanabe S, Ichiyama A, Ogawa Y. 2003. Control of oxalate formation from L-hydroxyproline in liver mitochondria. *J Am Soc Nephrol*. 14(4):939–946.

Vonheijne G, Steppuhn J, Herrmann RG. 1989. Domain-structure of mitochondrial and chloroplast targeting peptides. *Eur J Biochem*. 180:535–545.

Wang K, Zhao H. 2015. Birds generally carry a small repertoire of bitter taste receptor genes. *Genome Biol Evol*. 7(9):2705–2715.

Wilman H, Belmaker J, Simpson J, de la Rosa C, Rivadeneira MM, Jetz W. 2014. EltonTraits 1.0: species-level foraging attributes of the world's birds and mammals. *Ecology* 95(7):2027–2027.

Wilson DS, Yoshimura J. 1994. On the coexistence of specialists and generalists. *Am Nat*. 144(4):692–707.

Wilson MF. 1974. Avian community organization and habitat structure. *Ecology* 55:1017–1029.

Witmer MC. 1998. Ecological and evolutionary implications of energy and protein requirements of avian frugivores eating sugary diets. *Physiol Zool*. 71(6):599–610.

Yang Z. 2007. PAML 4: phylogenetic analysis by maximum likelihood. *Mol Biol Evol*. 24(8):1586–1591.

Zhang GJ, Li C, Li QY, Li B, Larkin DM, Lee C, Storz JF, Antunes A, Greenwold MJ, Meredith RW, et al. 2014. Comparative genomics reveals insights into avian genome evolution and adaptation. *Science* 346(6215):1311–1320.

Zhang J, Rosenberg HF, Nei M. 1998. Positive Darwinian selection after gene duplication in primate ribonuclease genes. *Proc Natl Acad Sci U S A*. 95(7):3708–3713.

Zhang J, Zhang YP, Rosenberg HF. 2002. Adaptive evolution of a duplicated pancreatic ribonuclease gene in a leaf-eating monkey. *Nat Genet*. 30(4):411–415.

Zhang X, Roe SM, Hou Y, Bartlam M, Rao Z, Pearl LH, Danpure CJ. 2003. Crystal structure of alanine: glyoxylate aminotransferase and the relationship between genotype and enzymatic phenotype in primary hyperoxaluria type 1. *J Mol Biol*. 331(3):643–652.